On the loading-rate dependence of the Al 7017-T73 fracture-initiation toughness

María Jesús Pérez-Martín , Borja Erice , Francisco Gálvez

Abstract

While static fracture toughness is a widely studied and standardised parameter, its dynamic counterpart has not been exhaustively examined. Therefore, in this research a series of quasi-static and different loading-rate dynamic tests were carried out to determine the evolution of fracture toughness with the velocity of the application of the load on aluminium 7017-T73 alloy.
Three-point bending tests of pre-fatigued standard specimens (ASTM E399) at four loading-rates were carried out. The experiments were conducted by employing the subsequent apparatus ordered from lowest to highest load application velocity: a servo-hydraulic universal testing machine, a free-drop tower, a modified Split Hopkinson Pressure Bar and an explosive load testing device. In order to perform the dynamic fracture toughness tests, it was necessary to design and develop some experimental devices. The fracture-initiation toughness of the aluminium 7017-T73 alloy did not exhibit a significant variation for the studied cases. As a conclusion, the research showed that fracture-initiation toughness remained constant regardless of the velocity at which the load was applied.

Keywords: Fracture-initiation toughness; loading-rate; free-drop tower; Split Hopkinson Pressure Bar; impulsive loading.

1. Introduction

In general, constitutive equations and failure criteria of materials depend on the strain rate. Therefore, in the case of materials that may be subjected to both low and high loading-rates it is crucial to be aware of how their fracture behaviour varies with the strain rate.

While static fracture toughness is a widely studied and standardised parameter (ASTM E399), obtaining such fracture toughness under dynamic conditions is somewhat complex because the specimen might not be under stress equilibrium. At present, there are no standards or guidelines to calculate the dynamic fracture toughness, though several methods, such as Rittel et al. (1992) or Weisbrod and Rittel (2000), are based on combining the stress-intensity factor history obtained from numerical simulations with the failure moment being determined from the experiments. Optical techniques and the coherent gradient sensing (CGS) method have also been used in dynamic fracture studies (e.g. Anderson et al. (2005)). Furthermore, several Hopkinson bar configurations and specimen geometries can be found, such as the following: three-point bending configuration (e.g. Gálvez et al. (2009) or Prasad and Kamat (2010)), semi-circular bend specimens (e.g. Dai et al. (2010)) or Charpy impact specimens (e.g. Fengchun et al. (2004) or Alexopoulos (2013)).

In this study a large experimental campaign was carried out in order to establish new experimental techniques that allow future calculation of fracture toughness at a wide range of loading rates. Therefore, three-point bending tests of pre-fatigued specimens at four loading-rates were carried out, employing a rate-independent aluminium alloy. Given that there was almost no difference identified among the fracture toughness values obtained for the different loading-rate, the proposed experimental techniques were validated.

The ASTM E399 standard describes the test method for plane-strain fracture toughness of metallic materials. This test method, in which fracture mode 1 is assumed, involves testing of notched specimens that have been fatigue pre-cracked, loading them either in tension or three-point bending configurations. Load versus displacement across the notch at the specimen edge is recorded. The fracture toughness value, K_{IC}, is calculated from this load by equations established on the basis of elastic stress analysis of specimens. The fracture toughness value characterizes the resistance of a material to fracture in the presence of a sharp crack under severe tensile constraint. If such a value is to be considered valid, the specimen thickness, B, and the crack length, a, should fulfil $B, a > 2.5\left(K_{IC}/\sigma_{YS}\right)^2$, being σ_{YS} the 0.2% offset yield strength of the material corresponding to the temperature and loading rate of the test.

There are several possible specimen configurations and the standard establishes the dimensions and the forms of fatigue crack starter notches. In this research, the bend specimen was chosen. In this case, the stress intensity factor, K_Q, should satisfy $K_Q = \left(P_Q S / BW^{3/2}\right) \cdot f\left(a/W\right)$. P_Q is a value of the measured load that should be determined according to the standards, S is the specimen span, W is the specimen width and $f(a/W)$ is a function defined with tabulated values in the standard. If $B, a > 2.5\left(K_Q/\sigma_{YS}\right)^2$ is satisfied, then K_Q is equal to K_{IC}.

As previously mentioned, the fracture toughness value of a given material may be a function of loading velocity and temperature. If this is the case, a different parameter should be defined. Such a parameter is the dynamic fracture-initiation toughness, K_{Id}. The crack starts to grow when the stress-intensity factor, $K_I(t)$, reaches a critical value, K_{Id}, which can be considered as a material property. Therefore, the dynamic fracture-initiation toughness can be calculated as, $K_{Id} = K_I(t_f)$, where t_f is the moment when the crack starts to grow. As in previous studies, such as Yokoyama (1993), Rubio et al. (2003) or Rubio-González (2008), in this research the dynamic fracture-initiation toughness values are compared with the corresponding value obtained under quasi-static loading conditions.

2. Material description

The material tested was an aluminium 7017-T73 alloy. The chemical composition in weight percentage and mechanical properties are summarised in Table 1. This alloy, one of the highest-strength aluminium alloys, contains zinc as the primary alloying element, magnesium which produces a marked improvement in precipitation hardening characteristics and chromium which provides an increase of the stress corrosion cracking resistance. The alloy was treated with a T73 heat-treatment, which consists of a heat-treatment solution and artificial aging that leaves the alloy beyond the point of maximum strength and achieves the best stress corrosion resistance.

Aluminium 7017 alloy is mainly used in armoured vehicles. This material was selected because its mechanical behaviour has been found to be nearly independent upon the strain rate (Rodríguez et al. (1994)).

Table 1. Certificated chemical composition and mechanical properties of aluminium 7017-T73 alloy

Chemical composition (weight %)							
Zn	Mg	Fe	Si	Cu	Mn	Cr	Zr
5.1	2.4	0.3	0.16	0.12	0.22	0.16	0.12

Mechanical properties (L-T orientation)			
E (GPa)	$\sigma_{0.2}$ (MPa)	σ_{UTS} (MPa)	ε_f (%)
71	450	499	12

3. Experiments

All the experiments were performed by employing the standard bend geometry. The standard bend specimen is a single edge-notched and fatigue cracked beam loaded in three-point bending configuration. A strain gauge was bonded close to the tip of the fatigue crack of each sample, enabling the measured strain to be associated with the load. This is considered as an indirect method of load measurement that is particularly important in the dynamic tests, given that they lack a load cell. In order to obtain the relationship between the applied load and measured strain, the pre-cracked sample was subjected to a loading and unloading cycle without any crack propagation. Such a relation was found to be linear and was different for every sample.

Three-point bending tests of pre-fatigued specimens at four loading-rates ($3 \cdot 10^{-6}$ m/s, 4 m/s, 10 m/s and 20 m/s) were carried out, employing the following apparatus: a servo-hydraulic universal testing machine, a free-drop tower, a modified Split Hopkinson Pressure Bar and an explosive load testing device. In order to perform tests at high load application velocity, it was necessary to design and develop new experimental devices.

3.1. Quasi-static tests

Four quasi-static fracture toughness tests were conducted in a servo-hydraulic universal testing machine at a load application velocity of $3 \cdot 10^{-6}$ m/s. These tests were carried out by following the recommendations of the standards. The experimental device used can be seen in Fig. 1(a). The specimen was positioned on two cylindrical roller bearings. Another cylinder, supported on top of the specimen, was the responsible of applying the load. Additionally, an extensometer with a range of +7/-1mm was attached to the specimen. The tests were recorded with a video camera configured to achieve 1 fps with a resolution of 2448x2048 px. The images were post-processed by employing digital image correlation (DIC) software provided by Correlated Solutions. The applied load was obtained by a 25 kN load cell and by the strain gauge measurement, that is, from the linear relation for each specimen.

3.2. Free-drop tower tests

Four three-point bending tests were conducted in a Dynatup 8250 free-drop tower at a load application velocity of 4 m/s. These tests were carried out by following the same distribution as the quasi-static tests. The experimental device used is shown in Fig. 1(b). The test consisted of dropping a 6 kg weight located 2 m above the specimen. A cylinder was attached to the bottom of the weight in order to apply the load. The specimen was positioned on two cylindrical roller bearings. The tests were recorded with a Phantom v12 high speed camera which was set to record at 180064 fps, taking 128x128 px resolution images with 5.55 μs spacing between each one. The DIC software was used to post-process the images. The equipment included high-powered lamps that were focussed on the specimen. The applied load was obtained by the strain gauge measurement, that is, from the linear relation for each specimen.

3.3. Modified Split Hopkinson Pressure Bar tests

Three fracture toughness tests were conducted in a modified Split Hopkinson Pressure Bar (SHPB) at a load application velocity of 10 m/s. A classical SHPB was modified in order to test the same specimen geometry as in the cases above. The test consisted of impacting the sample with an input bar. The experimental set-up showed in Fig. 2 was composed of a striker bar launched inside a tubular cannon and two input bars. The striker bar, made of steel, was 510 mm in length and 22 mm in diameter. The input bars, both of steel, were 1000 mm in length and 22 mm in diameter and had strain gauges attached in order to measure the incident and the reflected waves. In this case, the

end of the second input bar initially in contact with the specimen was rounded. The tests were recorded with a Phantom v12 high speed camera set to record at 120171 fps, leading a period of 8.32 μs among images, and with a resolution of 208x128 px. The images were post-processed by using the DIC software. The equipment included high-powered lamps focussed on the specimen. The load was obtained through applying the linear relationships calculated previously for each specimen to the measured strain from the strain gauge attached to the specimen.

The striker bar, launched with compressed air, impacted the first input bar. Such impact caused a compressive incident wave which travelled along the first and second input bars until it reached the specimen. As may be seen in the Fig. 2, in these tests cylindrical supports were not used. According to Chunhuan et al. (2011), during the initial loading phase there might be a loss of contact between the specimen and such supports. If the loss of contact time is greater than the time that the specimen takes to fracture, then there is no influence as regards the support conditions. This loss of contact has been reported previously in other studies, such as those by Yokoyama (1993) and Rubio-González et al. (2008).

3.4. Explosive tests

Fracture toughness tests were conducted under impulsive loadings by using explosives (see Fig. 3(a)). A new device was designed and developed to perform a three-point test under explosive loadings. The design was based on the ASTM E399 standard for the purpose of avoiding any influence of the way the device applied the load. Nevertheless, substantial modifications were made in order to adapt it to conduct tests under impulsive loadings. Four tests, divided in two sets, were carried out. For the first set 4.572 kg of TNT were used, producing a load application velocity of 20 m/s, for the second 3.325 kg were employed, reaching 13 m/s. Although the explosion generated a spherical wave, the rigid steel frame where the device was mounted allowed it to be treated as a plane wave (see Fig. 3(b)). The device shown in Fig. 3(c), allowed testing two specimens simultaneously. The specimens, positioned on two cylindrical roller bearings, were loaded when the wave reached the composite laminate shown in Fig. 3(b). A steel cylinder attached to it was applied the load. The laminate was composed of several carbon and glass-fibre plies. Due to the low weight of such a component, close to 0.4 kg, higher velocities could be achieved. Two coil springs were installed in order to guarantee that the load applier was initially in contact with the specimen. Two pressure transducers were used to measure the wave that reached the specimen. The load was obtained by converting the strain gauge measurement, with the linear relationship calibrated previously for each specimen.

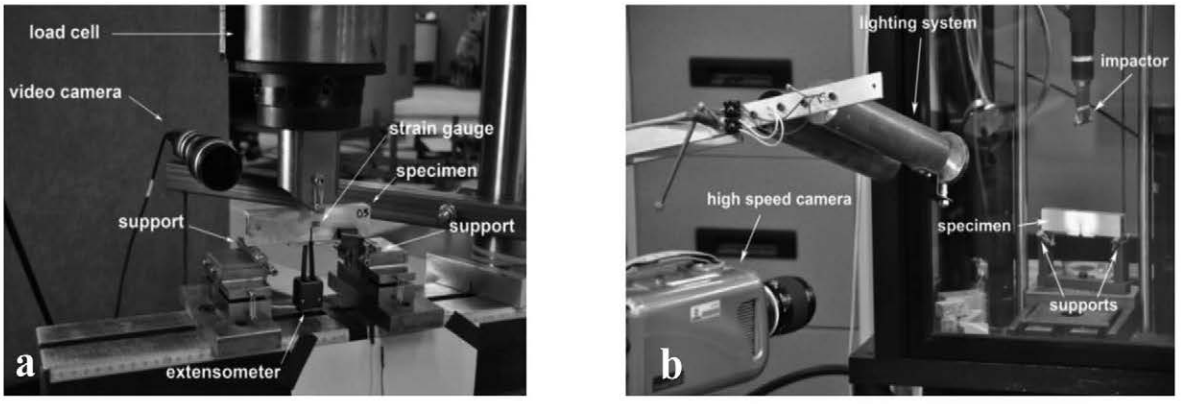

Fig. 1. (a) Experimental set-up for the quasi-static fracture toughness tests. (b) Experimental set-up for the free-drop tower tests.

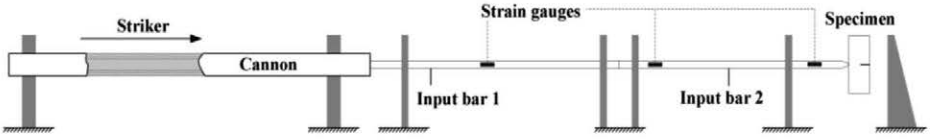

Fig. 2. Schematic view of the modified SHPB used to carry out the fracture toughness tests at a load application velocity of 10 m/s.

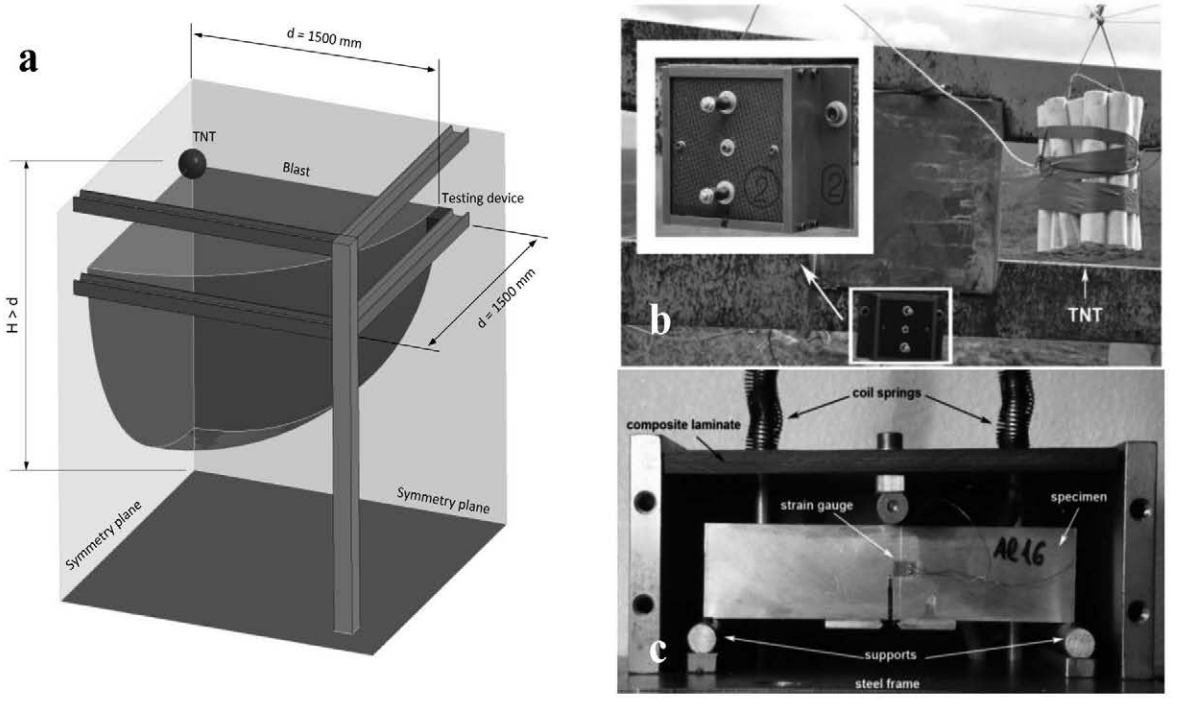

Fig. 3. (a) Experimental set-up for the explosive tests. (b) Specimen, with the strain gauge, positioned in the new device designed for explosive tests. (c) Detail of device attachment the steel frame employed for the tests under impulsive loadings.

4. Results

Under quasi-static loading conditions the applied load was obtained by the load cell, whereas under dynamic conditions it was obtained by operating the strain gauge measurement with the linear relationship calibrated specifically for each specimen. In the quasi-static tests, the strain histories were obtained through using three strain measuring techniques: the strain gauge, the extensometer and the DIC. All gave identical results. The DIC and the strain gauge measurements also coincided in the free-drop tower and the SHPB tests. Unfortunately, for the tests performed under impulsive loadings, due to the experimental set-up and landscape boundary conditions, only the strain gauge measurement was possible.

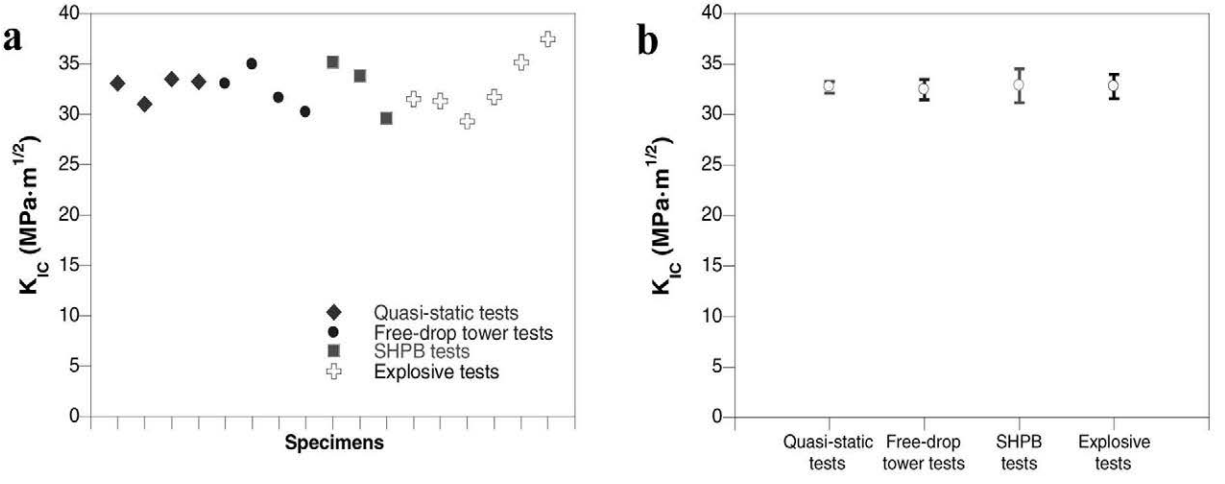

Fig. 4. Fracture toughness for aluminium 7017-T73 alloy: (a) all the specimens, (b) mean value and its standard deviation.

Once all the tests had been performed, the crack length for each specimen was measured. After checking that the requirements of the standards had been satisfied, the fracture toughness for each specimen was determined. Fracture toughness and dynamic fracture-initiation toughness values for the aluminium 7017-T73 alloy at four loading-rates are shown in Fig. 4(a). As shown in Fig. 4(b), the four devices provided a mean value of 33 $MPam^{1/2}$. The two "fastest" tests, SHPB tests and explosive tests, gave a slight scatter, whereas the two "slowest" ones, free-drop tower tests and quasi-static tests, revealed significantly lower variation. The possible misalignments between the bars and the specimen might be a plausible reason for the scatter encountered in the SHPB tests. In the case of the explosive tests, the scatter is easier to explain because of the nature of the experiments. In this case, the experiment was subjected to a non-regulated environment out of the laboratory. The explosive depended on the atmospheric conditions and landscape configuration, proof of which is the high scatter observed on the pressure histories measured by the transducers located in the steel frame employed in the experiments. Additionally, the wave that reached the testing device might not be completely spherical.

5. Conclusions

The research provided two main conclusions: the first was that the fracture-initiation toughness of the aluminium 7017-T73 alloy remained constant regardless of the velocity at which the load was applied; the second was that the four experimental devices provided the same value of the fracture-initiation toughness of the aluminium 7017-T73 alloy, with each being reliable devices for such a purpose.

In light of the obtained results, the test procedures under dynamic loading conditions were validated. That is to say, the test procedures determined the fracture-initiation toughness to a sufficiently accurate degree.

Acknowledgements

The authors would like to acknowledge the financial support of the Secretary of State for Research, Development and Innovation of the Spanish Ministry of Economy and Competitiveness through the project with reference BIA2011-24445.

References

Alexopoulos, N.D., Stylianos, A., Campbell J., 2013. Dynamic fracture toughness of Al-7Si-Mg (A357) aluminum alloy. Mechanics of Materials 58, 55-68.

Anderson, D.D., Rosakis, A.J., 2005. Comparison of three real time techniques for the measurement of dynamic fracture initiation toughness in metals. Engineering Fracture Mechanics 72, 535-555.

ASTM E399-12e3. Standard Test Method for Linear-Elastic Plane-Strain Fracture Toughness of Metallic Materials. Book of ASTM Standards Volume 03.01.

Chunhuan, G., Fengchun, J., Ruitang, L., Yang, Y., 2011. Size effect on the contact state between fracture specimen and supports in Hopkinson bar loaded fracture test. International Journal of Fracture 169, 77-84.

Dai, F., Chen, R., Xia, K. 2010. A semi-circular bend technique for determining dynamic fracture toughness. Experimental Mechanics 50, 783-791.

Fengchun, J., Ruitang, L., Xiaoxin, Z., Vecchio, K.S., Rohtgi, A., 2004. Evaluation of dynamic fracture toughness K_{Id} by Hopkinson pressure bar loaded instrumented Charpy impact test. Engineering Fracture Mechanics 71, 279-287.

Gálvez, F., Cendón, D., García, N., Enfedaque, A., Sánchez-Gálvez, V., 2009. Dynamic fracture toughness of a high strength armor steel. Engineering Failure Analysis 16, 2567-2575.

Prasad, K., Kamat, S.V., 2010. Dynamic fracture toughness of a near alpha titanium alloy Timetal 834. Journal of Alloys and Compounds 491, 237-241.

Rittel, D., Maigre, H., Bui, H.D., 1992. A new method for dynamic fracture toughness testing. Scripta Metallurgica et Materialia 26, 1593-1598.

Rubio, L., Fernández-Sáez, J., Navarro, C., 2003. Determination of dynamic fracture-initiation toughness using three-point bending tests in a modified Hopkinson pressure bar. Experimental Mechanics 43, 379-386.

Rubio-González, C., Gallardo-González, J.A., Mesmacque, G., Sánchez-Santana, U., 2008. Dynamic fracture toughness of pre-fatigued materials. International Journal of Fatigue 30, 1056-1064.

Weisbrod, G., Rittel, D., 2000. A method for dynamic fracture toughness determination using short beams. International Journal of Fracture 104, 89-103.

Yokoyama, T., 1993. Determination of dynamic fracture-initiation toughness using a novel impact bend test procedure. Journal of Pressure Vessel Technology 115, 389-397.